IEEE Access
Multidisciplinary : Rapid Review : Open Access Journal

Received December 9, 2018, accepted January 27, 2019, date of publication March 7, 2019, date of current version April 1, 2019.

Digital Object Identifier 10.1109/ACCESS.2019.2901936

A Fixed Miniaturization 90° Phase Shifter for VHF-Band High-Power Applications

NAIBO ZHANG[1,2], CHUNTING WANG[1], LEI LANG[1], AND JIANMING HUANG[2]
[1]54th Research Institute, China Electronics Technology Group Corporation (CETC54), Beijing 100070, China
[2]School of Electronic Engineering, Beijing University of Posts and Telecommunications, Beijing 100876, China

Corresponding author: Jianming Huang (ejmhuang@bupt.edu.cn)

This work was supported in part by the National Natural Science Foundation of China under Grant 61504124 and Grant 11635005.

ABSTRACT This paper presents a novel miniaturization 90° phase shifter using parallel coupled inductors and capacitors. The size reduction is achieved by replacing the quarter-wavelength transmission lines in a conventional fixed 90 degrees phase shifter with the resonator circuit. The resonator circuit, formed by the parallel coupled inductors and capacitor, provides a 90° phase shift at 45 MHz. In this way, the circuit size can be largely reduced without sacrificing the operation bandwidth and power handling. The inductors structure used in the phase shifter carries high power, which consists of two full coupled rectangle metal coils. The proposed miniature fixed phase shifter is then applied to the design of a directional coupler centered at 45 MHz. The measured results show a bandwidth of 40–50 MHz for better than 35 dB return loss with a phase shift of $\sim$ 90°, a deviation within $\sim$ 2°, and power handling of 63 dBm (2 kW). Notably, the proposed fixed phase shifter occupies an area of 58.5 mm $\times$ 30.5 mm $\times$ 33 mm, which is only about 0.009 $\lambda_0 \times$ 0.0045 $\lambda_0 \times$ 0.005 λ_0 at 45 MHz.

INDEX TERMS Phase shifter, directional coupler.

I. INTRODUCTION

PHASE shifters are widely used in microwave circuits and system, and are of great commercial and military interest [1]–[3]. For instance, phase shifters are important components with applications in phased arrays and smart antenna systems for fast and accurate beam forming and beam steering [4]–[7], and 3-dB directional coupler [8]. The conventional approach to design phase shifters is using the planar or micro-strip line or one of its variations that rely on the edge-coupled transmission lines. In recent years, the design of modified phase shifter circuits requires broader bandwidth, high return loss, and low phase-shift deviation, which proposed in [7], and [9]–[17]. In [9]–[12], the phase shifters are a cascade of the coupled sections. These configurations provide a wide bandwidth performance greater than 100%. However, the insertion loss and the size of phase shifter increase with an increasing number of the cascade sections.

Other structures [9], [15] proposed different configurations, rather than transmission lines. Such arrangement consists of basic and reference circuits using edge-coupled lines sections of different electric lengths and the same coupling coefficients, which provide less than 60% relative band width. A compact phase shifter [16] used the tapered coupled lines with a bandwidth higher than 80%, however, the phase shifters comprising edge coupled sections is limited by maximum coupling values of the edge coupled. The tight coupling requires a very narrow slot between the coupled lines, which is difficulty for fabrication. In [17] and [18], the compensation technique was introduced, numbers of capacitors were involved for the phase shifter structure. The results show that the technology improves the return loss performance, but it increases the insertion loss and has no effect on the bandwidth of the circuit. The digital switched phase shifter [19], [20] is a key component in microwave digitally controlled phased array antennas, which consists of a transmission-line branch and a bandpass filter branch. A 4-bit phase shifter was constructed with 22.5°, 45°, 90°, and 180° phase shifters, and the measured return loss was $\sim$ 14.5 dB and the insertion loss was $\sim$ 2.5dB. In [21]–[24], the structures consisted of micro-strip line, inverted phase micro-strip slot transitions and loaded air lines with inductor / resistor, a wide bandwidth performance greater than 100% was achieved, however, the size of phase shifter is large, which is approximately $\sim 0.2\lambda_0$ wave length at center frequency. In recent developments, some other technologies for phase shifters

The associate editor coordinating the review of this manuscript and approving it for publication was Roberto Gomez-Garcia.

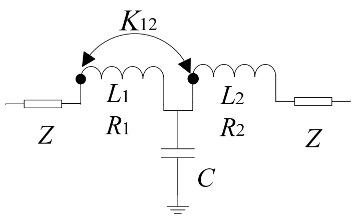

FIGURE 1. Phase shifter circuit, $L_1 = L_2 = 61.89$ nH, $R_1 = R_2 = 0.1\ \Omega$, $C = 202.1$ pF, $K_{12} = 1$, $Z = 35\Omega$.

are proposed [25]–[31], like reflective, active, liquid crystal polymer, metamaterials, and substrate integrated waveguide. However, all of those types have either a limited relative bandwidth (10%-40%) or a high insertion loss (2 to 5 dB), in addition, there are complex and expensive manufacturing processes [31]. Moreover, most reports [1]–[32] about phase shifter didn't consider the power handling.

This paper presents a 90° phase shifter which consists of parallel coupled inductor structure and capacitors. The design in this study focuses on miniaturization and high-power handling application with frequency from 40 MHz to 50 MHz, which is applied for VHF band directional coupler, high power handling switch and ultra-short-wave radar system. The main research work of this paper is to design the corresponding 90-degree phase shifter circuit by using the 90-degree phase shift characteristic of the resonator at the resonance frequency point, and calculate the parameters of the circuit quantitatively. The theoretical feasibility of the device carrying 2000 W power is analyzed, and the corresponding device structure is designed for high power capacity. Finally, the device is fabricated and tested. The test results show that the device provides a 90° phase shift with a deviation of $\sim 2°$, the size is of $\sim 0.009\ \lambda_0$, return loss is of < -35 dB and power handling is of 2000W. This paper also studies the application of this type phase shifter in directional coupler, which can also reduce the size of the device, have a large power handling and a good performance.

II. CIRCUITS DESIGN AND ANALYSES

The 1/4 wavelength transmission line was usually used for the traditional high-power 90-degree phase shifter, however, if the scheme is used for VHF band phase shifter, the device sizes will be very large. The circuit of inductors and capacitors is used for the small size of 90-degree phase shifter in this paper, and the principle is as: The resonator consisted of inductor and capacitor can produce an extreme value at the resonance point, which means that the slope at resonance frequency point is an infinite value, then the phase at the resonance frequency point is $\pi/4$ degrees. Therefore, the size of device is determined by the resonator size, not by the size of the 1/4 wavelength transmission line, and the circuit size is much smaller than the transmission line. In order to obtain the small size of resonator, the inductor and capacitor are adopted for designing the phase shifter. In order to further to reduce the resonator size, the circuit is designed as parallel coupled inductor and lumped capacitors, which is shown in Fig.1. The circuit is designed and simulated by software Advanced Design System (*ADS*), the parameters of circuit are calculated by following theoretical analysis and optimization simulation.

A. FORMULATION ANALYSES

An equivalent circuit is designed as Fig.1. The *ABCD* matrix is used for calculating circuit parameters.

$$\begin{bmatrix} A & B \\ C & D \end{bmatrix} = \begin{bmatrix} \cos\theta & jZ\sin\theta \\ j(1/Z)\sin\theta & \cos\theta \end{bmatrix} \begin{bmatrix} 1 & jwL_e \\ 0 & 1 \end{bmatrix} \begin{bmatrix} 1 & 0 \\ jwC & 1 \end{bmatrix} \times \begin{bmatrix} 1 & jwL_e \\ 0 & 1 \end{bmatrix} \begin{bmatrix} \cos\theta & jZ\sin\theta \\ j(1/Z)\sin\theta & \cos\theta \end{bmatrix} \quad (1)$$

where l is transmission line length, Z is the characteristic impedance, w is resonant frequency, L_e is inductor and C is capacitor in Fig.1. The electric length of transmission line is $\theta = 2\pi \cdot (l/\lambda)$. Because the length of transmission line (l) is defined as ~ 2 mm, the θ equals to 0.108 degrees, so the equation (1) can be expressed as,

$$\begin{bmatrix} A & B \\ C & D \end{bmatrix} \approx \begin{bmatrix} 1 & 1 \\ 0 & 0 \end{bmatrix} \begin{bmatrix} 1 & jwL_e \\ 0 & 1 \end{bmatrix} \begin{bmatrix} 1 & 0 \\ jwC & 1 \end{bmatrix} \begin{bmatrix} 1 & jwL_e \\ 0 & 1 \end{bmatrix} \begin{bmatrix} 1 & 0 \\ 0 & 1 \end{bmatrix} = \begin{bmatrix} 1 - wCL_e^2 & jwL_e(2 - w^2CL_e) \\ jwC & 1 - wCL_e^2 \end{bmatrix} \quad (2)$$

The S_{21} is obtained from equation (2), and expressed as,

$$S_{21} = \frac{2}{2 - 2w^2CL_e^2 + jw(C + 2L_e - w^2CL_e^2)} \quad (3)$$

When w is resonant frequency in equation (3), the relationship between C and L_e can be expressed as following,

$$C = \frac{1}{w^2L_e} \quad (4)$$

Substituting (4) into (2), and a quadratic equation of one variable with respect to L_e is obtained.

$$(jw^2S_{21} - 2S_{21})L_e^2 + (2wS_{21} - 2w)L_e + jS_{21} = 0 \quad (5)$$

Two solutions are obtained by solving the above equation, one of which is a negative solution and is neglected, and the solution (L_e) is as follows.

$$L_e = \frac{w(1 - S_{21}) + \sqrt{w^2(S_{21} - 1)^2 + S_{21}^2(w^2 + 2j)}}{S_{21}(jw^2 - 1)} \quad (6)$$

The parameters C and L_e can be solved by (4) and (6),

$$C = \frac{S_{21}(jw^2 - 1)}{w^3(1 - S_{21}) + w^2\sqrt{w^2(S_{21} - 1)^2 + S_{21}^2(w^2 + 2j)}} \quad (7)$$

In this study, a *L-C* circuit is used for the phase shifter. A characteristic impedance of $\sim 35\ \Omega$ ($50/\sqrt{2}\ \Omega$) is applied and provided as an example. The parameters L_e and C are obtained as 123.78 nH and 202.1 pF from equations (6)-(7), respectively.

B. CIRCUIT SIMULATION

In the Fig.1, the inductor L_1 equals to L_2, and two inductors are tightly coupled, the relationship between inductors L_e and $L_{1/2}$ is as following,

$$\begin{cases} L_e = L_{1/2} + M \\ M = K_{12}\sqrt{L_1 L_2} \end{cases} \tag{8}$$

where, M is mutual inductance coefficient, K_{12} is the coupling coefficient which equals to $K_{21} = 1$. The parameters in Fig.1 are calculated by equations (4)-(8), and Fig.2(a) shows the return loss of circuit by simulating the circuit, the figure shows ~ -85 dB return loss when center frequency is $\sim$ 45 MHz, Fig.2(b) is phase of insertion loss, the circuit provides a 90° phase shift at 45 MHz with a good linear characteristic from 40 MHz to 50 MHz.

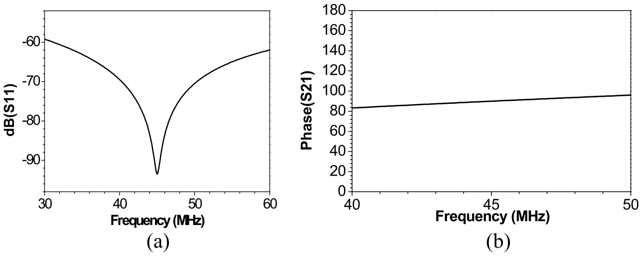

FIGURE 2. Performance of phase shifter circuit. (a) Return loss. (b) Variation of the phase shift with frequency.

III. STRUCTURE DESIGN AND ANALYSES

The phase shifter structure is designed by the circuit in Fig.1, two factors need to be considered: 1) the tightly coupled design of inductors, 2) the capacity of 2000 W power. In order to have a high power handling, metal sheets with a certain thickness are used to design inductors, and at the same time through analyzing the current distribution and resistance characteristics on the device, the device which has high power capacity are designed.

A. DESIGN STRUCTURE

In order to obtain a high-power handling, the phase shifter structure should have high current and low resistance at 45MHz. The metal strip side view is shown in Fig.3, which shows a diagram of the current distribution. Due to the skin effect of current, the current mainly distributes from r to r_0, and the current density is expressed as,

$$J = J_0 e^{-\alpha(r_0 - r)} \tag{9}$$

where, J_0 is surface current density, α is attenuation constant, r_0 is the outer diameter of current distribution, and r is the internal diameter of current distribution.

$$\alpha = \sqrt{\frac{w\mu\sigma}{2}} \tag{10}$$

where, w is frequency, σ is conductivity, μ is magnetic permeability, and the skin depth of current is given.

$$\Delta = \sqrt{\frac{2}{w\mu\sigma}} \tag{11}$$

The current consists of the current density integral of the whole plane,

$$I = \iint J_0 e^{-\alpha(r_0 - r)} dS = \iint J_0 (e^{-\alpha(x_0 - x)} + e^{-\alpha(y_0 - y)}) dS \approx \frac{1}{\sqrt{2}} \pi\sigma E_0 \frac{1}{\alpha} \sqrt{x_0^2 + y_0^2} = \frac{1}{\sqrt{2}} \pi\sigma E_0 \Delta \sqrt{x_0^2 + y_0^2} \tag{12}$$

where, x_0 and y_0 are border length, E_0 is equivalent electrostatic field.

$$R = \frac{E_0 l}{I} = \frac{l\sqrt{2}}{\pi\sigma\Delta\sqrt{x_0^2 + y_0^2}} = \frac{1}{7\sqrt{x_0^2 + y_0^2}} \tag{13}$$

where, l is unit length, when $R < 0.1\Omega$, $x_0^2 + y_0^2 = 2$. The parameters are designed as, $x_0 = 2$ mm, and $y_0 = 0.75$ mm, and then $R = 0.067\ \Omega$. When the power is up to 2000 W and the voltage is 220V, the current above is $\sim$ 9A. It's concluded from Ohm's law that the heat generated from the phase shifter is $\sim$ 5.4 W. Therefore, the phase shifter has a power handling of 63dBm (2000W).

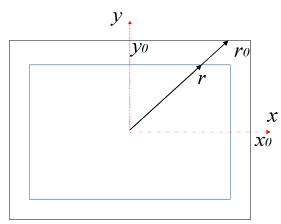

FIGURE 3. Side view of metal strip, and the skin effect of microwave transmission line.

In order to obtain the tightly coupled of inductors, the inductor structure is designed as two tightly coupled metal coils and shown in Fig.4, 1) One port of an inductor structure is input terminal, and the other port is connected with the other inductor port. 2) The remaining ports of two inductors are connected together. Two inductors are twined by a gap (b) for a high coupling coefficient. Two discrete capacitors are used for this phase shifter. The fixed 90° phase shifter consists of two parallel coupled inductors and capacitors. The parallel coupled inductors, which consist of two metal coils, is designed as four sides rectangle shape with the length h_2. Fig.4(a) shows the overall view of phase shifter structure, each inductor is constituted by 13 pieces metal strips, the strip has a length ($e + 2h_6$) and thickness h_6. There are three pieces strips in each three sides and four pieces strips in the other side. Each metal strip made for inductor has same sizes expect the four metal strips in the bottom side in Fig.4(b). The long metal strip consists of two rectangle structure and one parallelogram structure in Fig.4(b), and the parallelogram structure has an angle of θ_1. In order to connect two inductors,

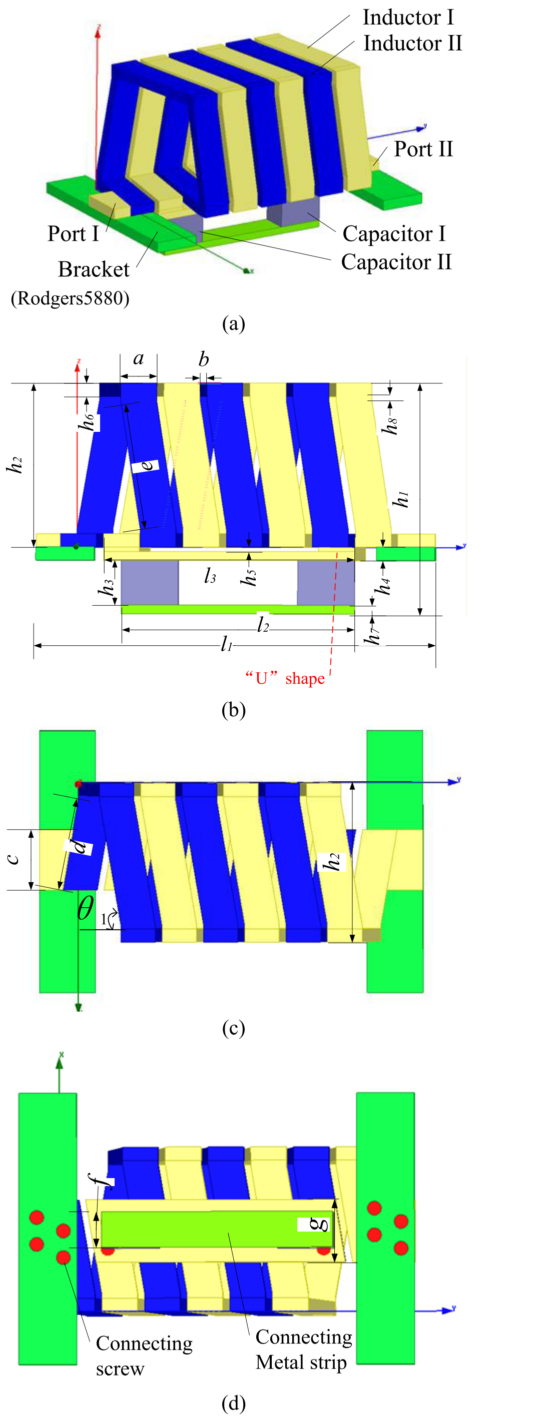

FIGURE 4. (a) Phase shifter structure. (b) Side view of phase shifter structure, $a = 4$ mm, $b = 0.8$ mm, $e = 14.6$ mm, $h_8 = 0.5$ mm, $l_1 = 44.5$ mm, $h_1 = 25.94$ mm, $h_2 = 17.94$ mm, $h_3 = 6$ mm, $h_4 = 1.5$ mm, $h_5 = 0.5$ mm, $h_6 = 1.5$ mm, $h_7 = 1$ mm, $l_2 = 26$ mm, $l_3 = 28$ mm. (c) Top view of phase shifter structures, $c = 7$ mm, $d = 10.65$ mm, $\theta_1 = 81°$. (d) Back view of phase shifter, $f = 4$ mm, $g = 7.1$ mm.

a "U" shape is designed as connecting bridge, which has length of l_3, gap of h_5, and width of c. The capacitor C is divided as two capacitors with capacitance of $C/2$, which is designed for the stability of whole structure. The two capacitors connect to the "U" shape structure, and the other side is connected to a metal strip with length of l_2, thickness of h_7 and width of c. To achieve a perfect coupling, two inductors are coupled with three turns and gap width of b. The whole size of phase shifter is l_1 the height is h_1, and capacitor height is h_3. And the phase shifter structure is packaged in a metal box with size of $\sim 58.5 \times 30.5 \times 33$ mm^3.

B. PARAMETERS OPTIMIZATION

In order to obtain good performances of phase shifter, the inductor parameters are analyzed. The inductor $L_{1/2}$ is determined by turns N, sectional area A, and length of inductor l. The formula is expressed as,

$$L_{1/2} = \frac{\mu_0 \mu_r N^2 A}{l} \tag{14}$$

where, μ_0 is permeability of free space and equals to $4\pi \times 10^{-7}$H/m, μ_r is relative permeability, A is the sectional area of inductor, and l is the total length of inductor wire. There is no core inside the inductor, the relative permeability μ_r equals to 1, inductor turns N equals to 3 in this paper, and the sectional area is a square shape, there is a relationship among sectional area A, length l and structure parameters, which are expressed as,

$$\begin{cases} A = h_2^2 \\ l = 11(h_2 - h_6) + 2d + h_6 \\ h_2 = 2(h_6 + h_8) + e \sin\theta_1 \end{cases} \tag{15}$$

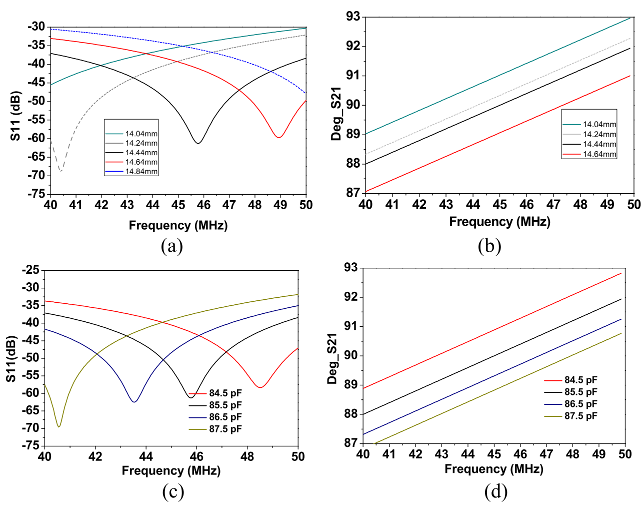

FIGURE 5. Simulated frequency responses of the proposed phase shifter (a) Return loss of phase shifter when inductor changes, (b) Variation of the phase shift with frequency. (c) Return loss of phase shifter when capacitor changes, (d) Variation of the phase shift with frequency.

According to formula (14) - (15) and optimization simulation, the parameters of inductor are obtained. When the inductor turns N and gap width b are defined, the inductor is determined by the metal strip length e, Fig.5 shows the phase shifter performances, Fig.5 (a)-(b) show the return loss and phase performances with different inductances.

When metal strip length e changes from 14.04 *mm* to 14.84 *mm*, the resonant frequency increases from 40 MHz to 50 MHz and phase decreases from 90.2° to 89.2° at 45 MHz. Fig.5 (c) - (d) show the return loss and phase performances with different capacitances. When capacitance changes from 84.5 pF to 87.5 pF, the resonant frequency decreases from 48.5 MHz to 40.5 MHz, and phase decreases from 90.5° to 88° at 45 MHz. The change of resonant frequency leads to the change of phase, the phase change caused by inductance is opposite to the phase change caused by capacitance.

IV. EXPERIMENTAL RESULTS

Fig.5 shows the fabricated phase shifter, which is formed by parallel coupled inductor, capacitors and bracket. The metal strip is fabricated by CNC milling process, and each metal strip is connected by cross dentate structure and shown in Fig.6(a). The width of metal strip ($a = 4$ mm) is divided into five pieces and used as cross dentate structure, each dentate structure width is designed as 0.8 mm. The bracket is designed as a circular structure which used for fixing the phase shifter, and the material is Rogers RT/duroid 5880, the material has little effect on the phase shifter performances. Fig.6(a)-(b) shows the fabricated inductors and capacitors, the capacitors are welded between "U" shape and bottom metal strip, and is connected with ground (package) by screws. The package and the detail sizes are shown in Fig.6(b)-(c). Fig.6(d) shows the power handing test setup schematic of phase shifter, the attenuator is ~ 50 dB, the test range of power meter is 20 dBm, test result is ~ 13 dBm, and the device has power handling of ~ 63dBm at least. Fig.7 is the comparisons between simulated results and measured results. In Fig.7(a), the test results show a good agreement with simulation results when frequency is from 40 MHz to 50 MHz, and a phase shift with 90° at 45MHz is achieved, the measured phase deviation is ~ 2° from 40 MHz to 50 MHz. The return loss in Fig.7(b) is less than −35 dB, the center frequency is ~ 45.5MHz. All results are tested by Agilent vector network analyzer (VNA) av3672b.

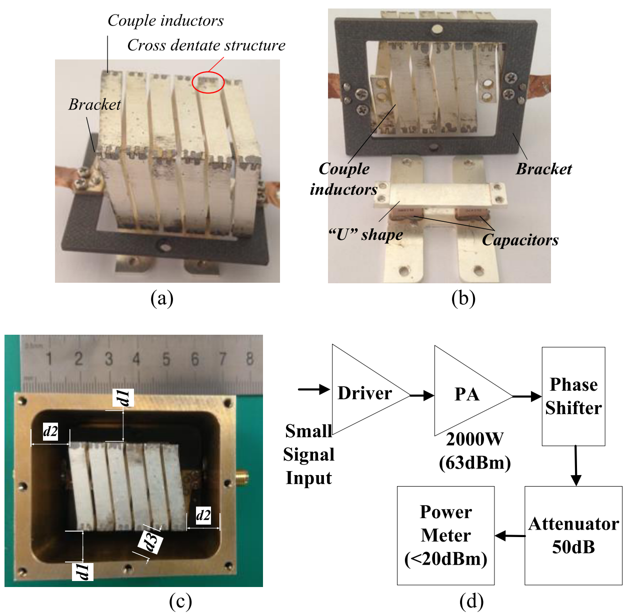

FIGURE 6. Fabricated phase shifter, (a) Parallel coupled inductor structure, (b) Structure detail, (c) Package shell with $d_1 = 6.25$ *mm*, $d_2 = 6.975$ *mm*, $d_3 = 7$ *mm*. (d) The power handing test setup schematic of phase shifter.

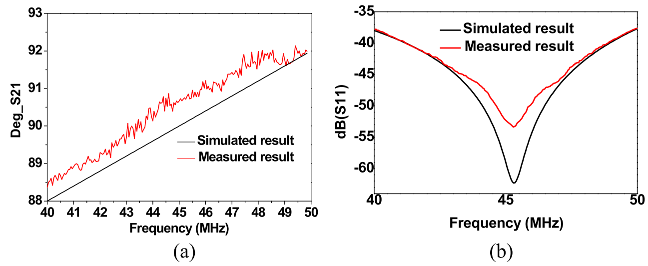

FIGURE 7. The comparison between simulated results and measured results. (a) Variation of the phase shift with frequency. (b) Return loss of phase shifter.

V. DISCUSSION AND APPLICATION

This study presents a fixed 90 degrees phase shifter by using parallel coupled inductors and capacitor. The size reduction is achieved by replacing the quarter-wavelength transmission lines in a conventional fixed 90 degrees phase shifter with the resonator circuit. In this way, the circuit size can be largely reduced without sacrificing the operation bandwidth and power handling. However, there are some problems when comparing the test results with the simulation results, and the corresponding discussion is as follows. In addition, this structure phase shifter can be well applied to directional couplers, which can greatly reduce the sizes and have high power carrying capacity, and the application is analyzed in the following. All optimization simulations are carried out by software *HFSS*.

A. DISCUSSION

The center frequency is designed as 45MHz, and the test result is 45.5MHz, there is a little deviation between simulation and test. The reasons are as following, 1) the lumped capacitor (202.1 pF) is divided into two capacitor (101 pF) in simulation, however, each capacitance is 100 pF in actual fabrication, 2) The coupling coefficient in circuit equals to 1, however, there are some deviations between simulation and test. Based on the above analysis, the center frequency has a deviation (~ 0.5 MHz). In addition, the bandwidth in this study is not as wide as proposed in [9], [10], [15], and [17], the function $\theta(w)$ in equation (3) is used for analysis.

$$\frac{d\theta}{dw} = \frac{d}{dw}\left\{\arctan\frac{w\left[(1+\frac{3}{Z})(w^2CL_e-2)-C\right]}{2(1+\frac{1}{Z})(1-w^2CL_e)}\right\} \tag{16}$$

In equation (16), the value of $|d\theta/dw|$ is proportional to the bandwidth. In this study, when the relative bandwidth

TABLE 1. Comparison between different types and configurations of phase shifters.

	Configuration	phase shift ($\Delta\Phi$)	Phase error (°)	Insertion loss $\lvert S_{21}\rvert$ (dB)	Return loss $\lvert S_{11}\rvert$ (dB)	Size in λ_0	Relative band width (BW/f_0)	Power handling (W)
Ref.[1]	"十" style micro strip	45°	± 4°	<1	>13	~ 0. 3 λ_0	~ 100%	—
Ref.[9]-[14]	Folded planar coupled line (CL) section $\lambda/4$	90° 45°, 180° 45°, 90°	± 5°	<2	>15	~ 0.07 λ_0 ~ 0.025 λ_0 ~ 0.023 λ_0	~ 66% ~ 50% ~ 40%	—
Ref.[12]-[13]	Cascaded and stepped multi section of planar CL	90°, 180°	± 5°	<1.5	>15	~ 0. 5 λ_0	~ 100%	—
Ref.[16]	Planar open ended coupled microstrip $\lambda/4$ section of the bandpass filter	45°, 135°	± 3°	<1	>15	~ 0. 3 λ_0	~ 40%	—
Ref.[17]	Planar topology using microstrip line with T shaped open stub	90°	± 3°	<1	>10	~ 0.066 λ_0	~ 82%	—
Ref.[19]	Transmission line bandpass filter with single pole double throw switched	4 bits (22.5°, 45°, 90°, 180°)	± 5°	2.5	14.5	—	~ 70%	—
Ref.[20]	Loaded transmission line with SPDT switches	45°	± 5°	2.2	15	~ 0.018 λ_0	~ 30%	—
Ref.[22]	Double in-phase and inverted-phase micro-strip slot transitions	±90°	± 8°	2	17	~ 0.4 λ_0	~110%	—
Ref.[25]	Micro-strip line	90°	± 5°	1.4	11.7	~ 0.218 λ_0	~50%	—
Ref.[26]	Loaded air lines, inductor, and resistor	90°	± 5°	_	_	~ 0.177 λ_0	~ 74%	—
Ref.[33]	Inductors and capacitors	90°	± 5°	<1	>20	~ 0.02 λ_0	—	100
Ref.[34]	Bridged T-coil.	90°	± 7.9°	<2	>15	~ 0.026 λ_0	~ 65%	—
Ref.[35]	Splitter, 65 *nm* COMS	90°	± 5°	<4	>10	~ 0.022 λ_0	—	—
Ref.[36]	LTCC	90°	—	<3	>10	~ 0.026 λ_0	**~ 55%**	—
This work	**Parallel coupled inductor and capacitors**	**90°**	± 5°	**< 1**	**>35**	**~ 0.009 λ_0**	**~ 50%**	**2000**

is $\sim 50\,\%$ (Extended from 35 to 55MHz) with phase deviations of ± 5° from Fig.7, the $|d\theta/dw|$ equals to $\sim$ 0.4 (°/ MHz) from equation (16). When the relative bandwidth is $\sim$ 100% with phase deviations of ± 5°, the $|d\theta/dw|$ equas to $\sim$ 0.2 (°/ MHz). For instance, if the relative bandwidth is $\sim$ 100%, the phase shifter circuit parameters are calculated as, $L_1 = 64$nH, $C = 207$pF, respectively. Therefore, bandwidth is inversely proportional to the value of $|d\theta/dw|$. In this study, the value of $|d\theta/dw|$ is larger than other papers [9], [10], [15], [17].

The benefits brought by the phase shifter structure (parallel coupled inductor and lumped capacitors) is, 1) in this paper, a phase shifter with small size is designed by using the characteristic that the resonator will produce 90 degrees phase shift at the resonant frequency point. As can be seen from Table 1, compared with the structural sizes in other literatures, the structures in this paper have very small sizes. 2) at the same time, the inductance formed by a certain thickness of metal sheet can bear high power characteristics.

To compare the proposed phase shifter in this study and reported phase shifters, Table 1 shows recently published phase shifter of 30°, 45°, 90°, 180°. Compared with phase shifters in literature [9]–[23], the proposed phase shifter provides a small size, a low loss $|S_{21}|$ and high return loss $|S_{11}|$ in operating frequency range. The proposed phase shifter can have both the advantages of a small size, a low insertion loss and high power handling in operating frequency range. Compared with phase shifter with the VHF frequency range [26], the phase shifter in this study shows a much smaller size and better performances than performances. When compare with [9], [12], and [25], the proposed filter in this study shows a higher return loss and s smaller size in defined band. These advantage features of proposed phase shifter will be useful for many system applications, such as, high power handling switch in VHF band, 3-dB coupler and ultra-short wave radar system.

B. APPLICATION

The phase shifter can be used for the directional coupler, and the coupler schematic is designed as Fig.8, which consists of four 90° phase shifter with $Z = 35\ \Omega$ and three 90° phase shifter with $Z = 121\ \Omega$. Port 1 is input, port 2 is isolated port, port 3 is through port, port 4 is coupled port, the phase difference equals to $\pi/2$ between port 3 and port 4.

The phase shifter circuit is the same as Fig.1. According to equations (3)-(4), when center frequency equals to 45 MHz, characteristic impedance Z equals to 121 Ω, the circuit parameters are obtained as, $L_1 = 214$ nH and $C = 58.46$ pF, respectively. The phase shifter structure is shown in Fig.9(a), the inductor is formed by metal strips and $N = 6$. The RF performances of phase shifter are shown in Fig.9(b). The return loss is less than −28 dB from 40 MHz to 50 MHz,

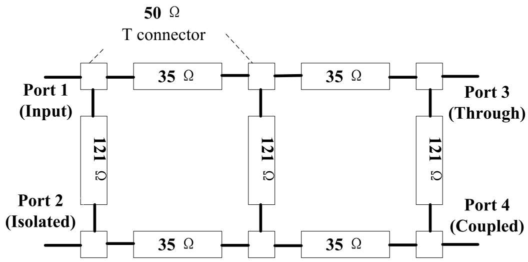

FIGURE 8. Schematic diagrams of directional coupler.

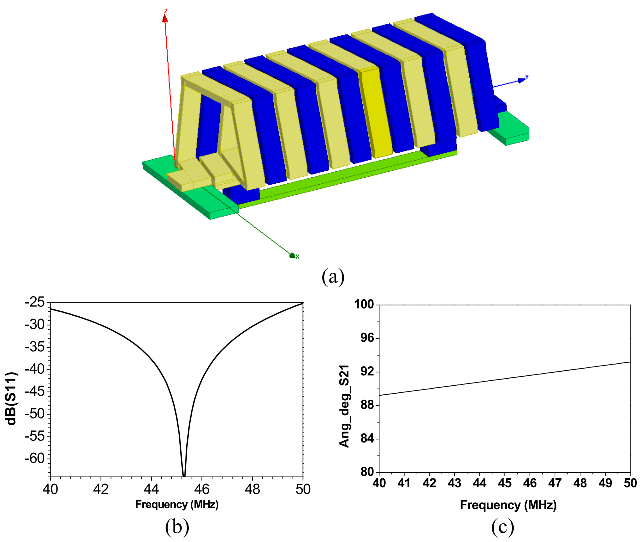

FIGURE 9. (a) Phase shifter structure when load impedance of 121 Ω. (b) Return loss of phase shifter, (c) Variation of the phase shift with frequency.

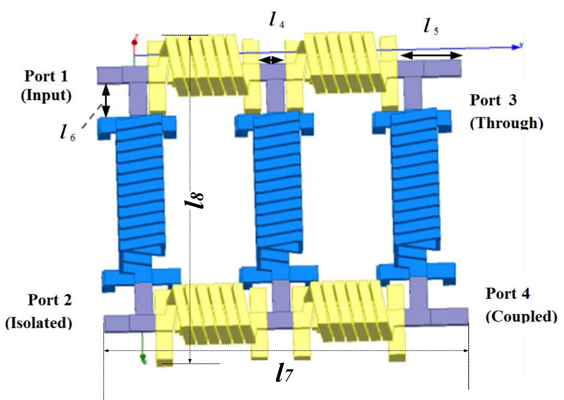

FIGURE 10. The model structure of directional coupler by using the fixed 90° miniaturization phase shifter.

and center frequency is ∼ 45 MHz. The phase shift is ∼ 90° when frequency is 45 MHz, and the maximum phase deviation is ∼ 2° from 40 MHz to 50 MHz. The fixed 90° phase shifter with 35 Ω and fixed 90° phase shifter with 121 Ω are designed for directional coupler. According to schematic diagrams in Fig.8, the coupler structure is formed by fixed phase shifters and connector structure, and is shown in Fig.10.

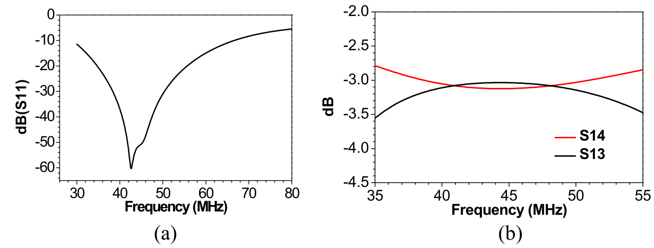

FIGURE 11. Performance of proposed directional coupler. (a) Return loss. (b) Insertion loss (S_{31} and S_{41}).

The connector structure is "T" shape, the sizes of "T" shape are: $l_4 = 14.1$ mm, $l_5 = l_6 = 24.1$ mm, $l_7 = 131.3$ mm, $l_8 = 110.5$ mm and the thickness is 1.5 mm. The package is made by metal material (copper) and the size is $145 \times 122 \times 33$ mm^3. Fig.11 shows the performance of the proposed coupler, which has a return loss of −50 dB at 45 MHz. The insertion loss S_{31} and S_{41} are $\sim (-3 \pm 0.5)$ dB from 38 MHz to 53 MHz, which means that half power is transferred from port 1 to port 3, the other half power is transferred from port 1 to port 4, and there is a 90 degree phase differences between port 3 and port 4, and is shown in Fig.11(b).

VI. CONCLUSION

This study presents a novel miniaturization 90° phase shifter by employing parallel coupled inductor and lumped capacitors. The phase shifter is designed for frequency range from 40 MHz to 50 MHz with a small size and a high power handling. The parallel coupled inductor is composed by two tightly coupled metal coils structures, which the parameters are extracted from equivalent circuit. A theoretical model is presented to explain the performance of this phase shifter and design procedure. Further, the phase shifter structure is designed and manufactured. The measured results showed good agreement with simulated results. The phase shifter provides a 90° phase shift at 45 MHz, the deviations of phase shift are ± 2° from 40 MHz to 50 MHz.

REFERENCES

[1] S. Y. Zheng and W. S. Chan, "Differential RF phase shifter with harmonic suppression," *IEEE Trans. Ind. Electron.*, vol. 61, no. 6, pp. 2891–2899, Jun. 2014.
[2] J.-L. Li and B.-Z. Wang, "Novel design of wilkinson power dividers with arbitrary power division ratios," *IEEE Trans. Ind. Electron.*, vol. 58, no. 6, pp. 2541–2546, Jun. 2011.
[3] S. Y. Zheng, W. S. Chan, and Y. S. Wong, "Reconfigurable RF quadrature patch hybrid coupler," *IEEE Trans. Ind. Electron.*, vol. 60, no. 8, pp. 3349–3359, Aug. 2013.
[4] H. L. Zhang, B. J. Hu, and X. Y. Zhang, "Compact equal and unequal dual-frequency power dividers based on composite right-/left-handed transmission lines," *IEEE Trans. Ind. Electron.*, vol. 59, no. 9, pp. 3464–3472, Sep. 2012.
[5] X. Y. Zhang, C. H. Chan, Q. Xue, and B.-J. Hu, "RF tunable bandstop filters with constant bandwidth based on a doublet configuration," *IEEE Trans. Ind. Electron.*, vol. 59, no. 2, pp. 1257–1265, Feb. 2012.
[6] K. Ma, R. M. Jayasuriya, and D. R. L. C. Siong, "Fully integrated high-isolation low-loss digitally controlled MEMS filters," *IEEE Trans. Ind. Electron.*, vol. 58, no. 7, pp. 2690–2696, Jul. 2011.

[7] H. R. Fang, X. Tang, K. Mouthaan, and R. Guinvarc'h, "180° and 90° reflection-type phase shifters using over-coupled lange couplers," *IEEE Trans. Microw. Theory Techn.*, vol. 60, no. 11, pp. 3440–3448, Nov. 2012.

[8] L. Chiu and Q. Xue, "Investigation of a Wideband 90° hybrid coupler with an arbitrary coupling level," *IEEE Trans. Microw. Theory Techn.*, vol. 58, no. 4, pp. 1022–1029, Apr. 2010.

[9] B. M. Schiffman, "A new class of broad-band microwave 90° phase shifters," *IRE Trans. Microw. Theory Tech.*, vol. 6, no. 2, pp. 232–237, Apr. 1958.

[10] B. Schiek and J. Kohler, "A method for broad-band matching of microstrip differential phase shifters," *IEEE Trans. Microw. Theory Techn.*, vol. MTT-25, no. 8, pp. 666–671, Aug. 1977.

[11] C. E. Free and C. S. Aitchison, "Improved analysis and design of coupled-line phase shifters," *IEEE Trans. Microw. Theory Techn.*, vol. 43, no. 9, pp. 2126–2131, Sep. 1995.

[12] V. Meschanov, I. V. Metelnikova, V. D. Tupikin, and G. G. Chumaevskaya, "A new structure of microwave ultrawide-band differential phase shifter," *IEEE Trans. Microw. Theory Techn.*, vol. 42, no. 5, pp. 762–765, May 1994.

[13] Y.-X. Guo, Z.-Y. Zhang, and L. C. Ong, "Improved wide-band Schiffman phase shifter," *IEEE Trans. Microw. Theory Techn.*, vol. 54, no. 3, pp. 1196–1200, Mar. 2006.

[14] G.-J. Sung, R. Kasim, J.-Y. Ryu, and B. Kim, "Broadband 180° bit-X-band phase shifter using parallel-coupled lines," in *Proc. Eur. Microw. Conf.*, vol. 3, Oct. 2005, pp. 319–321.

[15] J. L. R. Quirarte and J. P. Starski, "Novel Schiffman phase shifters," *IEEE Trans. Microw. Theory Techn.*, vol. 41, no. 1, pp. 9–14, Jan. 1993.

[16] P. Sobis, J. Stake, and A. Emrich, "High/low-impedance transmission-line and coupledline filter networks for differential phase shifters," *IET Microw., Antennas Propag.*, vol. 5, no. 4, pp. 386–392, Mar. 2011.

[17] S. Y. Zheng, W. S. Chan, and K. F. Man, "Broadband phase shifter using loaded transmission line," *IEEE Microw. Wireless Compon. Lett.*, vol. 20, no. 9, pp. 498–500, Sep. 2010.

[18] Z.-Y. Zhang, K. Wu, and Y. R. Wei, "Development of broadband phase shifter using slotted substrate integrated waveguide structure," in *Proc. IEEE Int. Ultra-Wideband Conf.*, vol. 1, Sep. 2010, pp. 1–4.

[19] X. Tang and K. Mouthaan, "Phase-shifter design using phase-slope alignment with grounded shunt λ/4 stubs," *IEEE Trans. Microw. Theory Techn.*, vol. 58, no. 6, pp. 1573–1583, Jun. 2010.

[20] X. Tang and K. Mouthaan, "Dual-band class III loaded-line phase shifters," in *Proc. Asia–Pacific Microw. Conf.*, Dec. 2010, pp. 1731–1734.

[21] M. Sorn, R. Lech, and J. Mazur, "Simulation and experiment of a compact wideband 90° differential phase shifter," *IEEE Trans. Microw. Theory Techn.*, vol. 60, no. 3, pp. 494–501, Mar. 2012.

[22] Y. Wang, M. E. Bialkowski, and A. M. Abbosh, "Double microstrip-slot transitions for broadband ±90° microstrip phase shifters," *IEEE Microw. Wireless Compon. Lett.*, vol. 22, no. 2, pp. 58–60, Feb. 2012.

[23] P.-S. Huang and H.-C. Lu, "Improvement of the phase shifter in 90° power splitter for UWB applications," *IEEE Microw. Wireless Compon. Lett.*, vol. 22, no. 12, pp. 621–623, Dec. 2012.

[24] C. Lee, "A new 90° constant phase shifter for the VHF band," *IEEE Trans. Commun.*, vol. COM-25, no. 12, pp. 1477–1480, Dec. 1977.

[25] K. Sellal, L. Talbi, T. A. Denidni, and J. Lebel, "Design and implementation of a substrate integrated waveguide phase shifter," *IET Microw. Antennas Propag.*, vol. 2, no. 2, pp. 194–199, Mar. 2008.

[26] Y. J. Cheng, W. Hong, and K. Wu, "Millimeter-wave multibeam antenna based on eight-port hybrid," *IEEE Microw. Wireless Compon. Lett.*, vol. 19, no. 4, pp. 212–214, Apr. 2009.

[27] Y. J. Cheng, W. Hong, and K. Wu, "Broadband self-compensating phase shifter combining delay line and equal-length unequal-width phaser," *IEEE Trans. Microw. Theory Techn.*, vol. 58, no. 1, pp. 203–210, Jan. 2010.

[28] C.-S. Lin, S.-F. Chang, and W.-C. Hsiao, "A full-360° reflection-type phase shifter with constant insertion loss," *IEEE Microw. Wireless Compon. Lett.*, vol. 18, no. 2, pp. 106–108, Feb. 2008.

[29] M. Hangai, M. Hieda, N. Yunoue, Y. Sasaki, and M. Miyazaki, "S-and C-band ultra-compact phase shifters based on all-pass networks," *IEEE Trans. Microw. Theory Techn.*, vol. 58, no. 1, pp. 41–47, Jan. 2010.

[30] F. Goelden, A. Gaebler, M. Goebel, A. Manabe, S. Mueller, and R. Jakoby, "Tunable liquid crystal phase shifter for microwave frequencies," *Electron. Lett.*, vol. 45, no. 13, pp. 686–687, Jun. 2009.

[31] P. He, J. Gao, C. T. Marinis, P. V. Parimi, C. Vittoria, and V. G. Harris, "A microstrip tunable negative refractive index metamaterial and phase shifter," *Appl. Phys. Lett.*, vol. 93, no. 19, pp. 193505-1–193505-3, 2008.

[32] A. M. Abbosh, "Broadband fixed phase shifters," *IEEE Microw. Wireless Compon. Lett.*, vol. 21, no. 1, pp. 22–24, Jan. 2011.

[33] T. Jun and W. Guoan, "Design of 30–150 MHz broad band bidirectional coupler," *Mod. Electron. Technol.*, vol. 35, no. 23, pp. 105–108, Dec. 2012.

[34] Y.-S. Lin and J.-H. Lee, "Miniature butler matrix design using glass-based thin-film integrated passive device technology for 2.5-GHz applications," *IEEE Trans. Microw. Theory Techn.*, vol. 61, no. 7, pp. 2594–2602, Jul. 2013.

[35] M. Ercoli, D. Dragomirescu, and R. Plana, "An extremely miniaturized ultra wide band 10–67 GHz power splitter in 65 nm CMOS technology," in *IEEE MTT-S Int. Microw. Symp. Dig.*, vol. 3, Jun. 2012, pp. 1–3.

[36] C.-H. Tseng, "Compact LTCC rat-race couplers using multilayered phase-delay and phase-advance T-equivalent sections," *IEEE Trans. Adv. Packag.*, vol. 33, no. 2, pp. 543–551, May 2010.

NAIBO ZHANG received the Ph.D. degree from the Beijing University of Posts and Telecommunications, Beijing, China, in 2012. From 2014 to 2016, he held a postdoctoral position with the University of Western Ontario, Canada. His current research interests include radio frequency filter, phase shifter. and antenna.

CHUNTING WANG received the Ph.D. degree from Xidian University, Xi'an, China. He is the Chief Expert of the China Electronic Science and technology. His research interests include telecommunication, RF circuits, and antenna.

LEI LANG was born in Shijiazhuang, China, in 1981. He received the B.Eng. degree (Hons.) in electronic information engineering from the Hebei University of Technology, Tianjin, China, in 2004, and the M.Sc. degree in electronic communications and computer engineering and the Ph.D. degree in electrical and electronic engineering from the University of Nottingham, Nottingham, U.K., in 2005 and 2011, respectively. Since 2012, he has been a Researcher with the CETC Networks and Communications Co. Ltd., where he was involved in several projects on the system design and implementation of visible light communications and free space optical communications. He was promoted to the position of Senior Engineer, in 2015. He has extended his research interests to wireless access technologies, near space information networks, and artificial intelligence application in communications. He has been involved in the National Science and Technology Expert Database, since 2018.

JIANMING HUANG received the Ph.D. degrees from Tsinghua University, in 1999, respectively. From 1999 to 2003, he was a Research Fellow with the School of Electrical and Electronic Engineering, Nanyang Technological University, Singapore. He currently is an Associate Professor with the School of Electronic Engineering, Beijing University of Posts and Telecommunications, Beijing, China. His current research interests include MEMS device and systems, especially RF and optical MEMS technology.